Bull. Astr. Soc. India (1993) **21**, 281-292

High resolution mapping in the far-infrared band

T. N. Rengarajan
Tata Institute of Fundamental Research, Homi Bhabha Road, Bombay 400 005

Abstract. The earth's atmosphere is opaque to the far-infrared (far-IR) radiation) and hence observations have to be carried out at altitudes above 12 km using telescopes transported by aircraft, balloon or satellite. The restriction to modest size telescopes in this environment along with the longer wavelengths of observations, results in poorer spatial resolution as compared to optical, near and mid infrared observations that can be made using ground based telescopes. However, the resolution of the far-IR observations has improved in recent times, with the employment of deconvolution techniques. This has led to significant results in several astrophysical situations in which the far-IR emission plays a major role. Some of these areas are protostars and outflow regions, sites of high mass star formation, star formation complexes in external galaxies and the relationship between far-IR emission and other indicators of star formation such as Hα and radio emitting HII regions, molecular hydrogen complexes and clouds of neutral hydrogen. This talk will describe some of the recent results obtained from high resolution studies in the far-IR and review the future prospects.

Key words : far-infrared—high resolution

1. Introduction

Higher and higher spatial resolution is an important goal of astronomical studies in order to probe, in greater detail, the astrophysical processes involved. The resolution possible in a given electromagnetic window depends on several factors like the wavelength, telescope size, the environmental condition and the detector technology. The far-infrared (far-IR) window has lagged behind other windows in many of the factors mentioned above. It is an important window covering over two decades in wavelength. We may conveniently take this window to be the one that is not accessible to ground based measurements i.e. from 25 μm to 300 μm. For some of our discussions, we will include the sub-mm wavelength up to 400 μm, though the 350-400 μm window is accessible from high mountain sites. The far-IR window is crucial for investigating the process of star formation. Stars form in dense cores of molecular clouds and in the early stages are deeply embedded in them. As a result, the luminosity of the underlying source is mostly absorbed by the surrounding dust which gets heated to temperatures of 20-100 K and radiate predominantly in the far-IR. The far-IR

observations, in conjunction with molecular line and thermal radio continuum observations have provided valuable insights into the process of star formation. In recent years, such studies have been extended to external galaxies also. There are many fundamental questions that need elucidation such as the fragmentation of molecular clouds leading to star formation, the star formation efficiency, the processes by which the low and high mass stars are formed, the initial mass function of stars formed, the impact of star formation on the molecular clouds and ISM etc. Before 1983, the far-IR observations came from aircraft and balloon borne telescopes. With the advent of the first space mission—the Infrared Astronomical Satellite (IRAS), the field has considerably widened. The IRAS mission made a complete unbiased all sky survey at four broad bands centered on 12, 25, 60 and 100 μm. Several studies based on the IRAS data and related observations in other electromagnetic windows have contributed richly to many fields. In this talk, I will be mainly concerned with the impact made by high resolution photometric observations in the far-IR. The present status of the resolution of far-IR observations will be reviewed and the astrophysical areas to which they make particular contribution will be enumerated. Some examples of high resolution studies and the astrophysical results obtained from them will be presented. Finally, I will end the talk with some comments on future prospects for this area.

2. Limitation on the resolution in the far-IR band

The diffraction limited resolution of a telescope is given by

$$\theta \text{ (arcsec)} = 0.25\ \lambda\ (\mu\text{m})/D(m) \qquad \ldots (1)$$

where λ is the wavelength of observation and D the diameter of the aperture. In the far-IR, the typical wavelength of 100 μm is much larger than in the optical and the near-IR resulting in much poorer resolution. Further, because of the opacity of the atmosphere to the far-IR wavelengths, telescopes have to be carried to the top of the atmosphere on aircrafts, balloons or satellites. Due to operational and launch difficulties, telescopes in such environments can have only moderate sizes, resulting in loss of resolution. For a typical ~1m diameter telescope used in aircrafts like Kuiper Airborne Observatory (KAO) and balloons, the resolution at 100 μm is 25 arcsec whereas for the 0.6m telescope on board the IRAS it is 42″. There is one narrow band of low atmospheric transmission in the 350-400 μm range accessible to telescopes at high and dry mountain sites. In this window one can then improve the resolution by having much larger mirrors. For example, sub 10″ resolution at 350-400 μm is obtainable with a telescope like the 15m JCMT in Mauna Kea. Prospects for telescopes larger than 2-3m in aircraft, balloon or space platforms are rather slim in the near future; improvement in resolution using interferometric technique is also far in the future.

The field of view (FOV) used in far-IR telescopes has generally been larger than the diffraction limit. In the IRAS mission this was dictated by the requirement of a complete survey. In the aircraft and balloon-borne telescopes, the pointing stability and the small throughput associated with diffraction limited FOV and the lack of array detectors with a large fill factors, have been the limitations. However, with well sampled data of sufficiently high *S/N*, one can obtain considerably better spatial information than defined by the FOV. Deconvolution techniques to get increased spatial resolution have been in use in radio astronomy for a long time. However, it is only in recent times, that such techniques have been used in

the far-IR field. The most commonly used technique is the one based on the Maximum Entropy Method (MEM) pioneered by Gull & Daniell (1978) and Skilling & Bryan (1984).

A major input to the MEM is the knowledge of the Point Spread Function (PSF), the response of the detector system to a point source. A reliable knowledge of the PSF up to reasonably low levels as compared to the peak response is essential for improving the spatial resolution and the dynamic range. In the MEM, the intensity distribution, is given by

$$S_i = \exp\left[-1 + 2\lambda \sum (E_j - G_j) \frac{P_{ij}}{\sigma_j^2}\right] \quad \ldots (2)$$

Here, the data are in a griddled form. S_i is the intensity at location i, E_j the observed signal at location j, σ_j the statistical error in E_j, P_{ij} the element of PSF relating signal at j to intensity at i, G_j the calculated signal at j for the estimated intensity matrix S and λ a positive multiplier. The procedure is iterative starting generally with a flat positive distribution and a small value of λ. As the iteration proceeds, λ is increased up to a maximum λ_{max}. To ensure convergence, intensity at any stage is taken as the weighted mean of the current iteration and the previous one. The MEM is dynamically driven in a 'direction' and 'rate' depending on a set of diagnostic parameters computed at the end of each iteration. Generally one needs to make simulations to arrive at appropriate values of the parameters involved.

Different authors have used several variants of the method appropriate to their data. Ghosh *et al.* (1988) have described the procedure adopted for the 2D deconvolution of balloon-borne chopped far-IR observations to get ~ 1′ resolution at 150 μm. Ghosh *et al.* (1993) have also deconvolved IRAS data using the mean PSF of detectors for each band and get a resolution of 1-2′. Lester, Harvey & Joy (1986a, 1986b) and their associates have extensively used ID MEM deconvolution techniques for their KAO observations to derive information on the far-IR sizes of compact sources (up to ~ 10 arcsec at 100 μm). Several techniques have been developed to get higher spatial information from the raw IRAS data which were taken with large non circular FOV's. The two procedures most often used are the ID ADDSCAN/SCANPI and 2D HIRES. In the former (Helou & Khan 1988) individual scan tracks are coadded to generate a mean scan profile. Using the known PSF along the inscan direction (narrower FOV) higher sensitivity and better resolution are obtained. HIRES is a more powerful 2D deconvolution routine employing the Maximum Correlation Method (Aumann, Fowler & Melnyk 1990). It is an iterative procedure which constructs models of the sky, uses the known IRAS detector response and scan tracks and compares the resulting image with the observed data. Details of the procedure and results are described in Aumann, Fowler & Melnyk (1990). After about 20 iterations, the routine achieves, or sources brighter than 1 Jy (or 2 MJy/Sr for extended sources), a resolution of 37 × 23, 35 × 23, 62 × 41, 98 × 80 arcsecs in the cross-scan × inscan direction for the 12, 25, 60 and 100 μm bands respectively. The HIRES routine is computer intensive. Ghosh *et al.* (1993, this issue) have shown that for bright sources the simple deconvolution procedure based on the mean detector PSF (instead of for the individual detectors) can be used, in much less computing time, to obtain maps of comparable resolution. However, the dynamic range is lower.

3. Astrophysics from high resolution far-IR studies

The far-IR band stretching over more than two decades in frequency is an important window for many astrophysical situations. In many situations, most of the luminosity of the source is in the far-IR band. With the advent of the unbiased all sky IRAS survey, samples of sources selected on the basis of far-IR characteristics are increasingly being used for several statistical studies. In this talk, we will however, be concerned mainly with those aspects where high resolution far-IR photometric studies can play an important role. Solar system studies will also not be discussed.

3.1. *Milky way*

Protostars : Emission from protostars is mainly in the far-IR. High resolution observations are crucial for identifying the protostar candidates, resolve them from the surrounding diffuse emission and determine their spectra. By comparing the observed spectrum with theoretical models, information on the nature of the source, presence of accretion disc, nature of the material surrounding the protostar etc. can be deduced.

Young low mass stars : These are often associated with bipolar outflows generally mapped in molecular lines. Quite often, the major luminosity is in the far-IR. High resolution observations help in determining the energetics of the energising source in the presence of other sources in the neighbourhood. Outflows are often associated with premain sequence objects and the far-IR studies in conjunction with the near-IR and molecular line observations, provide an insight into the evolutionary stage of these objects. The far-IR can also trace the dust and hence the matter around these sources.

High mass stars : The high mass stars are generally deeply embedded in their parent molecular clouds and as such most of their luminosity is re-radiated in the far-IR. They are also associated with ionizing HII regions and Hα emitting regions. The study of the dynamical interaction between the molecular clouds and the stars formed leading to a cycle of high mass condensates → high mass star formation → fragmentation of clouds will be greatly benefited by high resolution far-IR observations. A study of cloud complexes at different stages of evolution is of great interest. Another area of interest is the study of IMF of high mass stars from a combined study of far-IR emission (bolometric luminosity) and free-free radio continuum emission (Lyman continuum luminosity). High resolution in the far-IR is crucial for this, to distinguish between single stars and multiple stars.

3.2. *External galaxies*

Some of the areas on which major impact will be made by high resolution far-IR observations are :

(a) Mapping of star forming complexes, spiral arm structures etc. and comparison with similar maps of (i) molecular hydrogen (CO) complexes, (the sites of star formation); (ii) atomic hydrogen clouds (reservoir of gas); (iii) Hα emission (indicators of high mass star formation); (iv) radio continuum (HII region complexes and non thermal electrons in the ISM originating from high mass stars). These will probe the star formation process and their history and the relative contribution of high mass stars and intermediate mass stars to the far-IR luminosity.

(b) Investigations of the relative role of dust in the star forming complexes and in the ISM.

(c) Radial profile of far-IR emission and its relationship to radial profiles in other windows.

(d) Star burst phenomenon and the star forming efficiency of molecular cloud complexes.

(e) Relationship between interaction and star formation in galaxies.

(f) The nature of ultra luminous ($L > 10^{11.5} L_{\odot}$) galaxies and their relationship to galaxies containing AGN.

(g) Compact non-thermal sources in centres of active galaxies.

4. Results

In this section a few examples of high resolution far-IR studies and the results obtained will be described. Only a brief summary of the salient results of a few representative studies will be presented. For details one may refer to references cited.

4.1. *Star forming regions in the Milky Way*

Several star forming complexes in the Galaxy have been mapped by the TIFR group using their 1m balloon-borne telescope, at a long wavelength band centered on 150 μm. The resolution obtained is 1-1.5 arc min. The mapping at longer wavelengths traces the cool dust and gives more complete information on the luminosities. Figure 1 shows the 150 μm map of the W31 complex (Ghosh *et al.* 1989) while figure 2 shows the 150 μm map of the Carina complex containing η Car (Ghosh *et al.* 1988). In both complexes several compact sources superposed on a diffuse emission are seen. While the sources in W31 are mostly deeply embedded, and have no visible OB stars, in the Carina Complex there is more diffuse emission, the sources are weaker and there is a large number of visible OB stars. In the Carina complex many dusty clumps seem to be heated externally and the far-IR luminosity is only a few percent of the OB star luminosity in the region. These two complexes represent two different stages of evolution—W31 being the younger complex with deeply embedded OB stars while Carina is more evolved and the associated cloud has already fragmented a lot. The initial mass function of high mass stars derived for the young cluster Tr16 in the Carina complex is found to be flatter than that derived for W31 using the resolved radio continuum sources.

4.2. *Low mass star L1551 IRS5*

L1551 IRS5 is a low mass star in the Taurus dark cloud and has an associated bipolar outflow and is embedded inside a molecular core. High resolution far-IR observations which can provide information on the size, spectrum and the nature of dust are crucial for understanding models of their formation. Butner *et al.* (1991) have observed this source using the scanning photometer aboard the KAO. The scanning technique has been described by Lester, Harvey and Joy (1986a; 1986b). Repeated scans are made across the source using a slit FOV and 80-100 such scans are coadded. This scan profile is then deconvolved using a ID MEM. Scans are generally done in two perpendicular directions. Butner *et al.* (1991) have also used a linear array of ^{3}He cooled bolometers for obtaining the scan profile. By using the PSF obtained from scans of Callisto they find that L1551 IRS5 is slightly resolved at 100 μm,

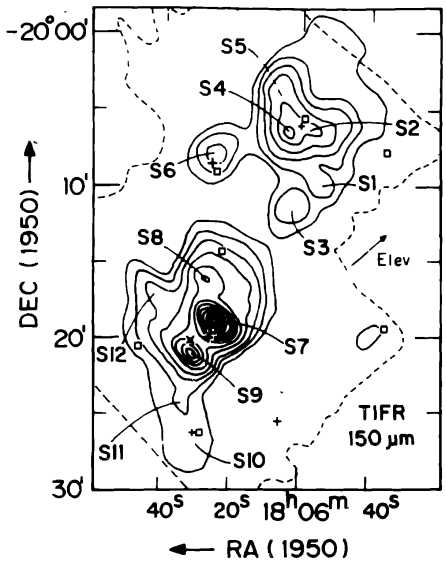

Figure 1. The 150 μm intensity map of W31 obtained using the TIFR 1 m balloon-borne telescope. The peak intensity is 3676 Jy/arc min^2 and the contours are 0.95, 0.9, 0.8, 0.7, 0.6, 0.5, 0.4, 0.3, 0.4, 0.1, 0.05, 0.025 and 0.01 of the peak. S1-S12 are sources identified; plus sign shows IRAS source position and the boxes, 5 GHz sources. (Reproduction of figure 1 of Ghosh *et al* 1989).

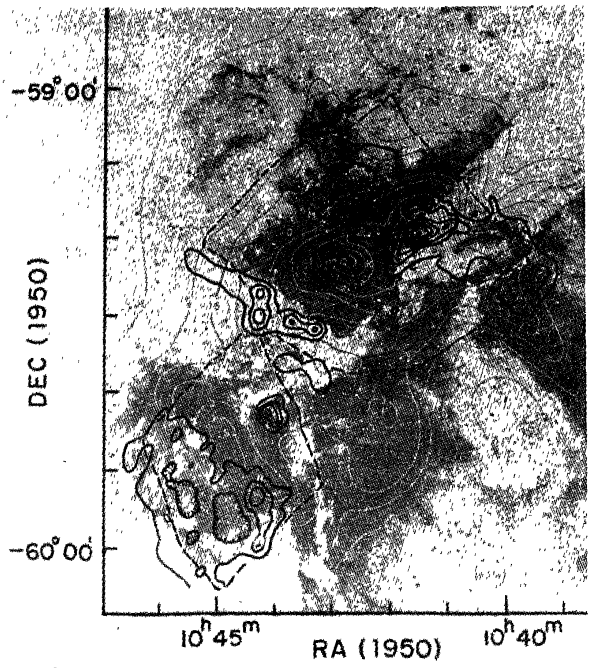

Figure 2. 120-300 μm map superposed on an optical photograph of the Carina region. The lighter contours are from the 5 GHz radio continuum (4′) observations. The peak far-IR intensity is 2000 JY/arcmin^2, while the contours are at 0.95, 0.5, 0.3, 0.1, 0.05 and 0.01 of the peak. (Reproduced from figure 4 of Ghosh *et al.* 1988).

giving a deconvolved size of ~ 11″, while at 50 μm it is unresolved. By combining their observation with those of others including the mm interferometric data of Keene & Masson (1990), they construct the spectrum of the compact source which is shown in figure 3. From this figure it is seen that there are deviations at the short and long wavelengths. Changes in dust properties cannot explain these deviations. The far-IR to mm spectrum along with the observed size at the mm wavelengths, implies the presence of a compact source, presumably a disc. Comparing with models, constraints are also placed on the density gradient of the surrounding dust and the best fit is that of $n(r) \propto r^{-1.5}$, consistent with the expectation for an infalling envelope (Adams Lada & Shu 1987). The size determination and spectrum of the compact source at the mm and far-IR wavelengths have been crucial for these conclusions.

4.3. *Far-IR and Hα emission in spiral galaxies*

There is disagreement amongst different workers as to the relative contribution of dust heated by high mass stars in the star forming complexes and the dust in the ISM heated by the radiation field. While mapping at ~ 200 μm to trace the cool dust would be valuable for this, one can also infer this information from a correlative study of far-IR and Hα maps, since Hα emission mainly arises from regions ionised by high mass stars. IRAS HIRES maps of face-on galaxies are ideal for this study. Rengarajan *et al.* (1993, in this issue) find that for NGC 6946 and NGC 4321 there are good spatial correlations between the Hα and the far-IR maps. The higher resolution possible at 25 μm makes this band a valuable tool for such studies. Devereux & Young (1992) have made quantitative comparison between the Hα and

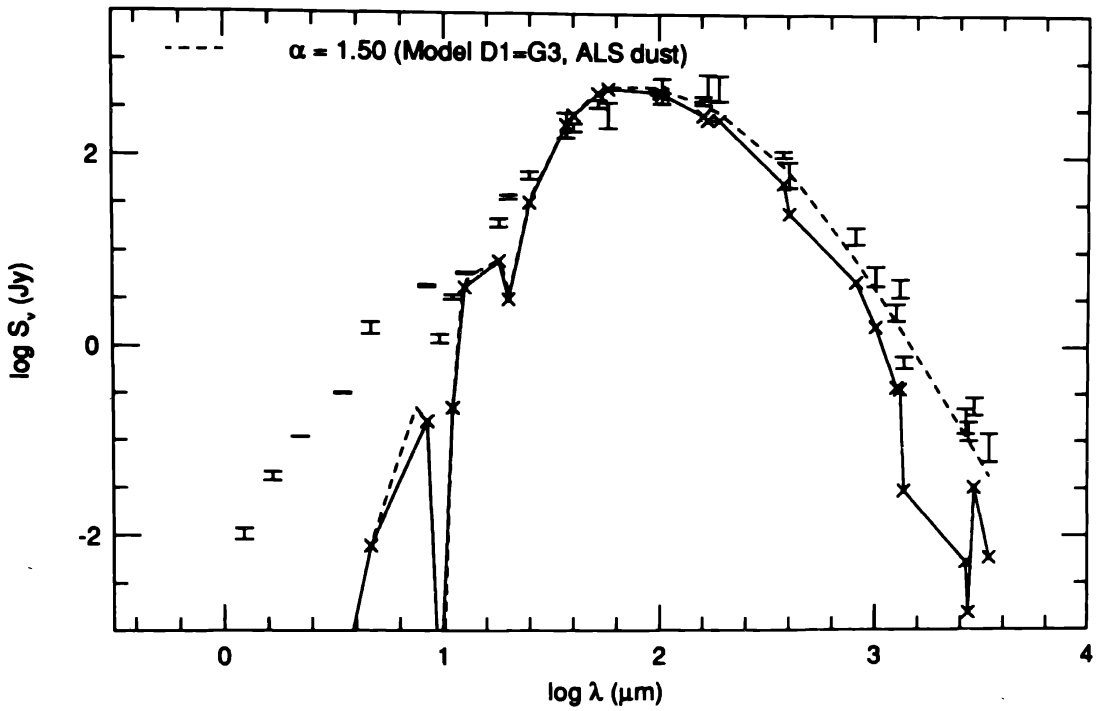

Figure 3. The spectrum of L1551 IRS5. The dashed line is the model prediction for a $r^{-1.5}$ density gradient for the circumnuclear material. The Xs are the fluxes that the model predicts for beam size used in the observation and are joined by solid line for visual aid only. (Reproduced from figure 10 of Butner *et al* 1991).

far-IR emission maps of M51 and conclude that the high mass stars are the dominant sources of dust heating. Figure 4, taken from their paper shows for M51, the azimuthally averaged radial distribution of L(FIR), (using the 160 μm map of Smith 1982), L(Hα), σ(H_2) and σ(HI). It is clearly seen that the first three are almost parallel indicating common spatial origin while the HI distribution is quite different.

4.4. *Mapping of cool dust in spiral galaxies*

Stark *et al.* (1989) have made use of the University of Chicago 32 element FIR Camera to map several Virgo galaxies at 160 μm using the KAO and at 360 μm using the IRTF, Hawaii. The closely packed detectors have a FOV of 45″ and a separation of 48″. Figure 5 taken from their paper shows a typical example. The bottom half shows the sampling of the field by the detectors and the top half shows the 160 μm and 360 μm maps for NGC 4254. Observations in the 350-400 μm window and the air borne far-IR observations in the 100-200 μm range can be a powerful combination to obtain high resolution images and investigate the role of cool dust.

4.5. *Interacting galaxy Arp 299*

Interacting galaxies are associated with high star formation activity and high star formation efficiency. Interferometric observations can now provide high resolution (~ 5″) mapping of these galaxies in the molecular lines of CO. Since the far-IR is the best indicator of star formation in these galaxies, high resolution observations at these wavelengths are very

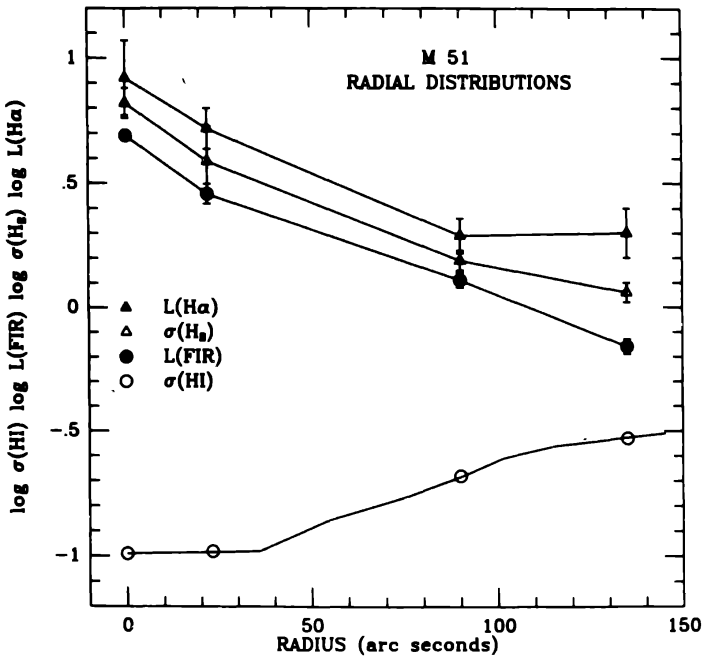

Figure 4. Azimuthally averaged radial distribution of the far-IR luminosity, L(FIR) measured in a 49″ beam, Hα luminosity, L(Hα) in 45″ beam, molecular gas surface density $\sigma(H_2)$ and the atomic hydrogen surface density, σ(HI). Luminosities are in units of $L_\odot$ and surface densities in $M_\odot$ pc^{-2}. (Figure 2 of Devereux & Young 1992).

fruitful. Joy *et al.* (1989) have investigated the Arp 299 system consisting of the pair NGC 3690 and IC 394 using the scanning photometer onboard the KAO. Simultaneous measurements were made at 50 μm and 100 μm using FOV's of 12″ × 40″ and 24″ × 40″ respectively (the narrower FOV corresponding to the diffraction limit). Several scans were coadded and the resulting profile was deconvolved using ID MEM. Figure 6 shows the observed profiles in the East-West direction at 50 and 100 μm. Also shown is the PSF. The two galaxies are clearly separated. While IC 694 is unresolved and has 60% of the far-IR luminosity, NGC 3690 is slightly resolved. Figure 7 shows the 50 μm scan profile along with a 20 μm scan profile. It is seen that the fainter NGC 3690 has the hotter 20-50 μm colour. The observed temperature gradient is opposite to that expected if the putative nucleus in IC 394 generates significant fraction of the total luminosity.

4.6. *Interacting galaxies—HIRES maps*

Surace *et al.* (1993) have very effectively used the ADDSCAN and HIRES techniques to resolve the multiple components of interacting galaxies. Their sample is from the sample of Bright IRAS galaxies and selected on the basis of optical morphology indicating interaction, but not mergers. The galaxies were also chosen such that the component separation is roughly along the IRAS scan track, the direction of best resolution. Figure 8 shows the example of Arp 271 wherein the two galaxies are clearly seen separated in the HIRES maps both at 60 μm and 100 μm. Also shown are model simulations. This study is the largest investigation with the best HIRES resolution for small angular size galaxies. Of the sample of 56 systems, 22 were resolved yielding a total of 51 galaxies. By comparing this interacting sample with a sample of isolated galaxies, the authors find that "even during the early stages

of interaction spanned by these systems, tidal perturbations appear to substantially boost far-infrared indicators of star formation compared to non-interacting systems".

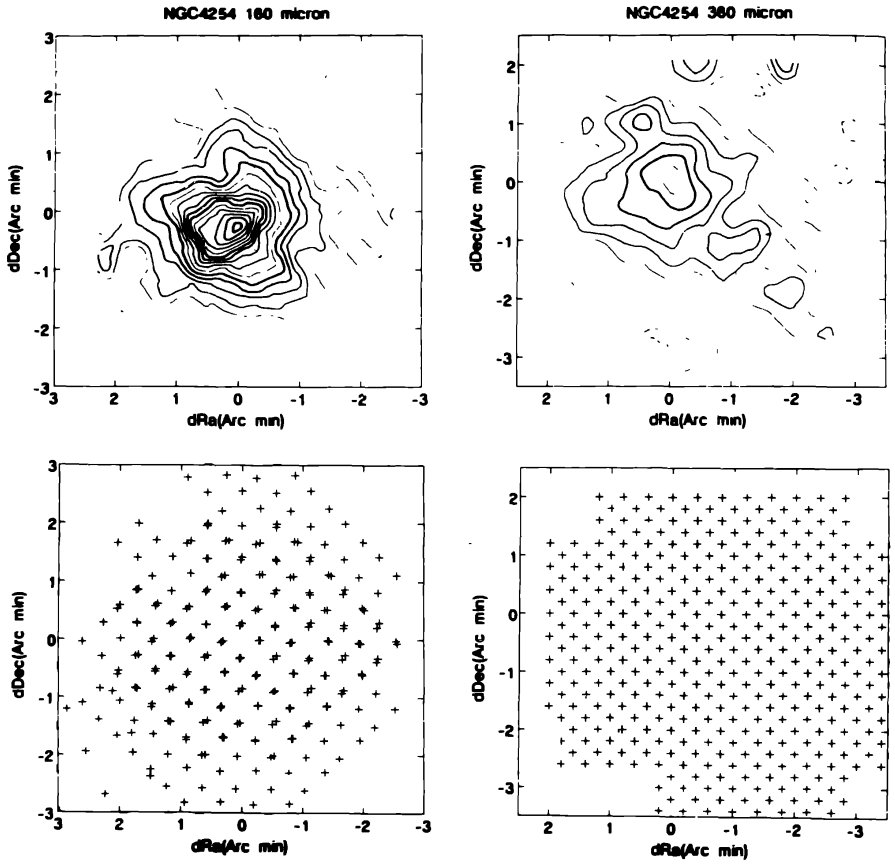

Figure 5. Maps at 160 μm and 360 μm of NGC 4254. Contours of 160 μm flux density are in units of 1.9 Jy/arc min^2 and of 360 μm flux density in units of 2.4 Jy/arc min^2. The lower panels : positions sampled by the arrays. (Reproduced from figure 1 of Stark *et al.* 1981).

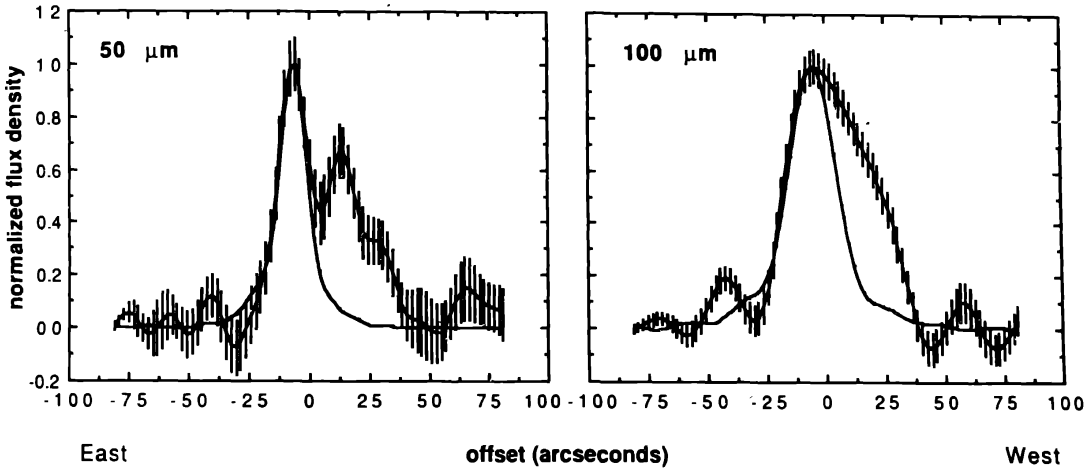

Figure 6. Coadded 50 μm and 100 μm profiles along the major axis of Arp 299 system. 54 individual scans were coadded . The error bar represents standard deviation of the mean at each point and the solid line shows the PSF. (Figure 1 of Joy *et al.* 1989).

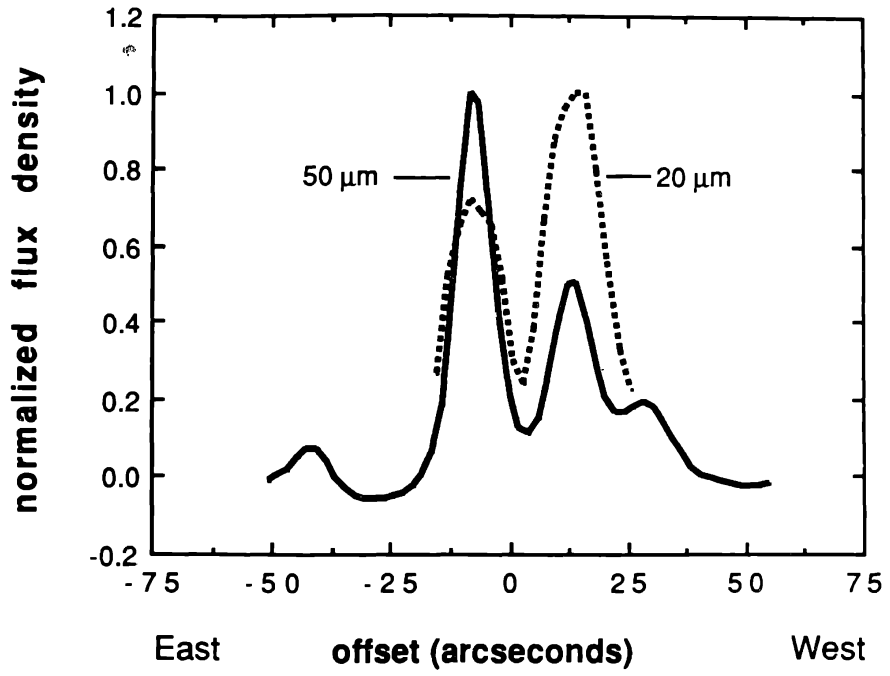

Figure 7. Beam matched 20 μm and 50 μm profile of Arp 299. The 20 μm image was numerically convolved with a matching 12″ × 40″ aperture for comparison with 50 μm profile (Figure 4 of Joy *et al.* 1989).

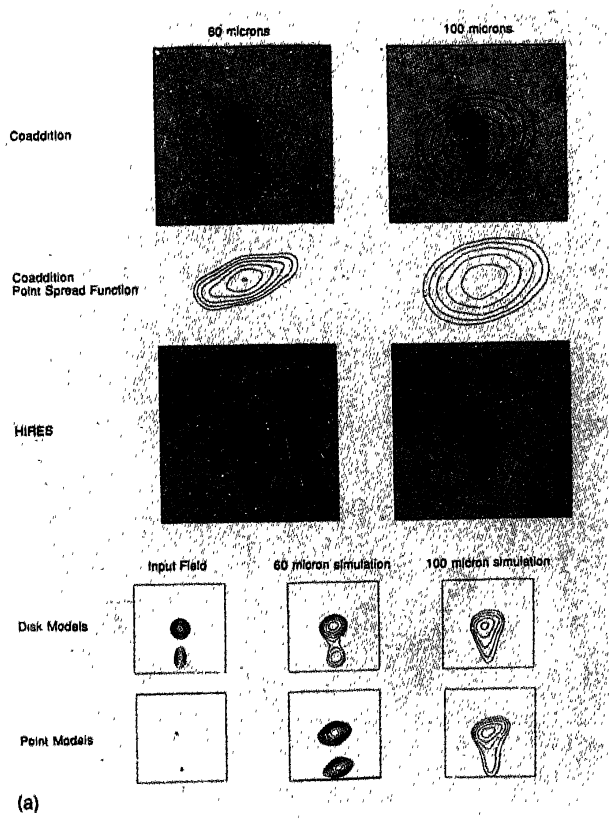

Figure 8. HIRES map at 60 and 100 μm of Arp 271 superposed on an optical photograph. Also shown are the point spread functions for coaddition and in the upper left, that for HIRES. Simulation for input field models are shown in the lower panels (Figure 1a of Surace *et al.* 1993).

4.7. *Non-thermal nuclear emission from NGC 5128*

Many radio galaxies have a compact non-thermal source. The far-IR and sub-mm region of the spectrum of the nuclear source is generally uncertain because of lack of resolution. However, this range is important for understanding the nature of the source, since turnover in the spectrum is expected in this range. Sub 10″ mapping in the 350 μm window and interferometric observations at 800 μm combined with high resolution far-IR measurement are now feasible and provide an opportunity to distinguish the nuclear source from the extended disc emission, resolve any circumnuclear structure and give a picture of the extended disc structure in dust. Hawarden *et al.* (1993) have carried out such a study on NGC 5128 (Centaurus A). They have used the high resolution capability of the 15m JCMT to obtain fully sampled maps at 450 μm and 800 μm and multi-aperture photometry at 1100, 1300 and 2000 μm. The spectrum is shown in figure 9. They clearly distinguish the unresolved nuclear source (< 6″) at both 800 and 450 μm. At 800 μm small scale (~ 30″) extension of the nuclear source presumably a dense dusty torus is also seen. Using the flux densities determined for the nuclear source and combining these with small beam observations at the far-IR wavelengths, they clearly establish that the spectrum of the nuclear source is flat and continues to be flat up to ~ 400 μm suggesting the presence of a blazar.

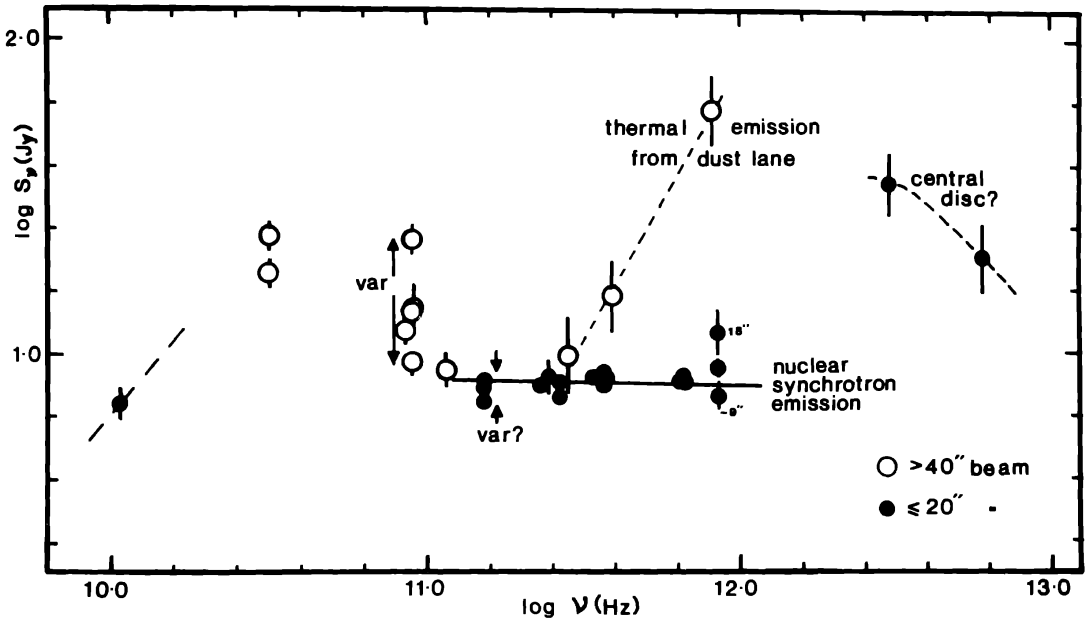

Figure 9. Spectrum of Cen A from 50 μm to 10 mm. Small beam measurements are separately shown. The flat spectrum for the small beam data and the presence of one or two more distinct spectral components may be noted (Figure 3 of Hawarden *et al.* 1993).

5. Future prospects

In the near future, there will not be large improvements in sizes of space-borne telescopes. The Infrared Space Observatory to be launched by the European Space Agency in 1995, will be more sensitive than the IRAS and will cover wavelengths up to 200 μm. It will be an object oriented mission. The mirror size is about the same as in the IRAS. However, the smaller FOV's and improvements in technique would lead to a better resolution, especially

for bright sources. The long awaited Space Infrared Telescope Facility of NASA is unlikely to be launched before the year 2000. Here again, though there will be a large improvement in sensitivity, the increase in resolution in the far-IR will be modest because of the sub 1m telescope size. As for the aircraft-borne telescope, there are proposals for flying 2.5-3m size telescope. This telescope, if and when funded and completed would have the best resolution in the far-IR, for a decade or more. As for the balloon-borne telescope, the TIFR group will continue to do long wavelength photometric mapping with a new ^{3}He cooled 12 detector array which is expected to give a resolution of 45″ in the 100-200 μm range. The French group at Toulouse have built a 2m balloon-borne telescope which is expected to be in regular use soon. This will provide, probably the best far-IR resolution till the end of the century. By employing specialised scan techniques and sophisticated procedures, it will be possible to reach sub 10″ resolution for specific bright sources. The prospects for the 350-400 μm window are brighter. The JCMT will continue to be used for the best resolution. The proposed sub-mm array of the Smithsonian Astrophysical Observatory, when completed in the next few years, will offer arcsec resolution opening up entirely new areas of investigations. Sub-mm observations will also benefit from telescopes that are planned to be operated from high sites in Antarctica, where during winter, the atmospheric conditions are the most favourable. In the mean time, a combination of the best resolution in the 100-200 μm, 350 μm observations and the ever increasing interferometric measurements at 800-1000 μm will play a major role in unravelling the mysteries of the dusty, cold and compact sources.

References

Adams F. C., Lada C. J., Shu F. H., 1987, ApJ, 312, 788.

Aumann H. H., Fowler J. W., Melnyk M., 1990, AJ, 99, 1674.

Butner H. N., Evans N. J., Lester D. F., Levreault R. M., Strom S. E., 1991, ApJ, 376, 636.

Devereux N. A., Young J. S., 1992, AJ, 103, 1536.

Ghosh S. K., Iyengar K. V. K., Rengarajan T. N., Tandon S. N., Verma R. P., Daniel R. R., Ho P. T. P., 1988, ApJ, 330, 928.

Ghosh S. K., Iyengar K. V. K., Rengarajan T. N., Tandon S. N., Verma R. P., Daniel R. R., 1989, ApJ, 347, 338.

Ghosh S. K., Das B., Rengarajan T. N., Verma R. P., 1993, BASI, 21, Nos. 3&4.

Gull S. F., Daniel G. J., 1978, Nature, 272, 686.

Hawarden T. B., Sandell G., Mathews H. G., Friberg P., Watt G. D., Smith P. A., 1993, MNRAS, 260, 844.

Helou G., Khan I., 1986, All about ADDSCAN, Infrared Processing & Analysis Centre, Pasadena.

Joy M., Lester D. F., Harvey P. M., Telesco C. M., Decher R., Rickard L. J., Bushouse H., 1989, ApJ, 339, 100.

Keene J., Masson C. R., 1990, ApJ, 355, 635.

Lester D. F., Harvey P. M., Joy M., 1986a, ApJ, 302, 280.

Lester D. F., Harvey P. M., Joy M., 1986b, ApJ, 304, 623.

Rengarajan T. N., Ghosh S. K., Verma R. P., 1993, BASI.

Smith J., 1982, ApJ, 261, 463.

Stark A. A., Davidson J. A., Harper D. A., Pernic R., Loewenstein R., Platt S., Engargiola G., Casey S., 1989, ApJ, 337, 650.

Skilling J., Bryan R. K., 1984, MNRAS, 211, 111.

Surace J. A., Mazzarella J. M., Soifer B. T., Wehrle A. E., 1993, AJ, 105, 864.